Electronic Journal of Biotechnology 78 (2025) 86–95

Contents lists available at ScienceDirect

Electronic Journal of Biotechnology

journal homepage: www.elsevier.com/locate/ejbt

Research article

METTL16 promotes osteosarcoma progression by inducing m^{6}A methylation of the UBE3A and Notch signaling pathway ☆

Yanlin Tan [a], Jun Gao [b,*]

[a] Department of Pediatrics, Wuhan Third Hospital, Wuhan, Hubei, China
[b] Department of Orthopaedics, The Third People's Hospital of Hubei Province, Wuhan, Hubei, China

GRAPHICAL ABSTRACT

METTL16 promotes osteosarcoma progression by inducing m^{6}A methylation of the UBE3A and Notch signaling pathway.

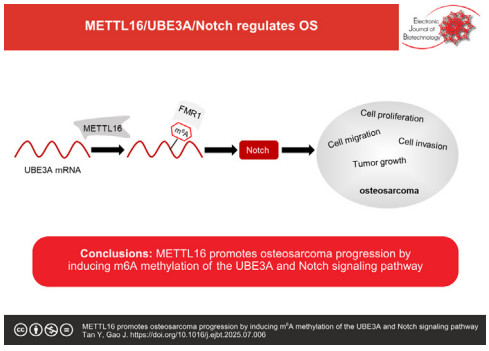

ARTICLE INFO

Article history:
Received 28 April 2025
Accepted 31 July 2025
Available online 9 October 2025

Keywords:
Bone tumor
m^{6}A
Methylation
Methyltransferase
METTL16
Notch signaling pathway
Osteosarcoma
Tumor promotor
UBE3A

ABSTRACT

Background: N6-methyladenosine (m^{6}A) methylation plays a key role in osteosarcoma (OS) progression. This study aimed to elucidate the function and mechanism of methyltransferase 16 (METTL16), an m^{6}A methyltransferase, in OS progression.

Results: Bioinformatics analysis with quantitative reverse-transcription polymerase chain reaction (qRT-PCR) revealed high METTL16 expression in OS. After performing cell functional experiments, METTL16 silencing was shown to decrease the proliferation, migration, and invasion of OS cells. Using qRT-PCR, methylated RNA immunoprecipitation quantitative polymerase chain reaction (MeRIP-qPCR), Western blotting, luciferase, RNA-binding protein immunoprecipitation (RIP), and RNA stability assays, METTL16 induced the m^{6}A methylation of ubiquitin protein ligase E3A (UBE3A) to promote UBE3A expression and mRNA stability in OS cells in a fragile X messenger ribonucleoprotein 1 (FMR1)-dependent manner. Moreover, *in vitro* and *in vivo* results showed that UBE3A activated the Notch signaling pathway, thereby promoting OS cell malignancy. METTL16 knockdown partly reversed the oncogenic role of UBE3A in OS cells.

Conclusions: METTL16 acts as a tumor promotor in OS progression by modulating UBE3A expression via m^{6}A methylation to activate the Notch signaling pathway. The findings highlight the therapeutic potential of disrupting the METTL16–UBE3A–Notch pathway axis in OS.

☆ Audio abstract available in Supplementary material.

Peer review under responsibility of Pontificia Universidad Católica de Valparaíso.

* Corresponding author.
E-mail address: gaojunhandsome@126.com (J. Gao).

https://doi.org/10.1016/j.ejbt.2025.07.006

How to cite: Tan Y, Gao J. METTL16 promotes osteosarcoma progression by inducing m6A methylation of the UBE3A and Notch signaling pathway. Electron J Biotechnol 2025;78. https://doi.org/10.1016/j.ejbt.2025.07.006.

1. Introduction

Osteosarcoma (OS), a malignant bone tumor, predominantly affects children, adolescents, and young adults [1]. Despite advancements in multimodal therapeutic strategies including surgery, chemotherapy, and radiation, the prognosis of patients with metastatic or recurrent OS remains dismal, with 5-year survival rates of 20–30% [2,3]. The aggressive nature of OS is driven by its propensity for early metastasis, resistance to conventional therapies, and lack of effective targeted drug options [4,5,6]. These challenges underscore the urgent need to elucidate the molecular mechanisms underlying OS pathogenesis, which may be necessary to identify novel targets for OS therapy.

Recent studies have highlighted epigenetic modifications as critical regulators of cancer progression, with N6-methyladenosine (m^6A) methylation being a pivotal post-transcriptional modulator of gene expression [7,8]. In eukaryotic mRNA, m^6A can dynamically regulate RNA splicing, stability, translation, and decay, thereby influencing diverse cellular processes [9,10]. The dynamic regulation of m^6A is catalyzed by a conserved set of "writer" proteins, including METTL3, METTL14, and METTL16, whereas its removal is mediated by "erasers" such as FTO and ALKBH5 [11,12,13]. Methyltransferase 16 (METTL16), a recently identified m^6A methyltransferase, has garnered increasing attention for its role in regulating mRNA methylation in cancer. For instance, METTL16 acts as an oncogene in breast cancer by inducing m^6A methylation of GPX4 mRNA [14]. In pancreatic cancer, METTL16 attenuates tumor growth and metastasis by promoting MROH8 mRNA stability [15]. This duality indicates that METTL16 plays different roles in specific cancers; however, its contributions to OS remain poorly characterized.

Ubiquitination, a posttranslational modification mediated by E3 ubiquitin ligases such as ubiquitin protein ligase E3A (UBE3A), governs protein degradation, DNA repair, and cell cycle progression [16,17,18]. Recent studies have revealed that UBE3A plays key roles in human diseases, particularly cancer. For example, UBE3A deletion in non-small-cell lung cancer improves the efficiency of immunotherapy [19]. UBE3A is an oncogene in esophageal cancer that activates the Notch pathway [20]. These studies on UBE3A in cancer indicate the oncogenic role of UBE3A in cancer. However, its function and regulatory mechanism in OS are unknown.

This study aimed to investigate the role and mechanism of METTL16-mediated m^6A methylation of UBE3A in OS progression via *in vivo* and *in vitro* experiments. We hypothesized that METTL16 induces the m^6A methylation of UBE3A to regulate UBE3A mRNA stability, thereby participating in OS progression. Our results not only expand the understanding of m^6A biology in OS but also identify METTL16 as a promising therapeutic target.

2. Materials and methods

2.1. Bioinformatic analysis

TNMplot (https://tnmplot.com/analysis/) is an online platform for analyzing METTL16 expression across normal and OS tissues. GSE16088, an mRNA microarray from GEO DataSets, stores differentially expressed genes (DEGs) across normal and OS tissues. With $\log_2FC > 2$ and adj. $p < 0.01$, the upregulated DEGs in OS samples were screened, whereas TNMplot predicted the METTL16-correlated genes in OS. Venny 2.1 was applied to overlap common genes in GSE16088 and TNMplot.

2.2. Cell culture and Notch inhibitor DAPT treatment

The human osteoblast cell line hFOB1.19 (BFN6072012687) was provided by BlueFBio (China), whereas two human osteoblast cell lines, U2OS (SNL-054) and HOS (SNL-480), were provided by Suncell (China). hFOB1.19 and HOS were cultured in Dulbecco's Modified Eagle Medium +10% fetal bovine serum (FBS), whereas U2OS was cultured in McCoy's 5a medium +10% FBS. The cell culture was performed in an incubator (5% CO_2 and 37°C). As for DAPT, 25 μM DAPT, a Notch inhibitor, was purchased from Selleck (China) and added to OS cells for treatment for cell culture.

2.3. Quantitative reverse-transcription polymerase chain reaction (qRT-PCR)

The EasyPure RNA Kit (TransGen, China) was added to cell or tissue samples to obtain the total RNA. qRT-PCR was performed using Green One-Step qRT-PCR SuperMix (TransGen) with 100 ng of RNA and primers (0.2 μM forward and 0.2 μM reverse primers) listed in Table 1. GAPDH was used as an internal control to calculate the relative expression of METTL16, UBE3A, and SON.

2.4. Cell transfection

To silence METTL16 expression, small interfering RNAs targeting METTL16 (si-METTL16#1 and si-METTL16#2) were synthesized by GenScript (China). A UBE3A overexpression vector was constructed by GenScript using pcDNA3.1, and empty pcDNA3.1 (empty vector) was used as a negative control. OS cells were transfected with the abovementioned vectors using Lipofectamine 3000 (Invitrogen, USA).

2.5. OS cell proliferation assessment

Cell Counting Kit-8 (CCK8, Yeason, China) was used to assess changes in OS cell proliferation. Briefly, 2000 OS cells per well after transfection were seeded into 96-well plates. At 0, 24, 48, and 72 h after seeding, 10 μL CCK8 was added to each well for 1 h of incubation. A microplate reader was used to read the absorbance of each well at 450 nm.

Table 1
Qrt-pcr primer sequences.

Gene name	Sequence
METTL16	Forward 5′-TGGAGCAACCTTGAATGGCTGG-3′
	Reverse 5′-CCATCAGGAGTGTCTTCTGTGG-3′
UBE3A	Forward 5′-CCCTGATGATGTGTCTGTGG-3′
	Reverse 5′-GGCAAAGCCATTTCCAGATA-3′
SON	Forward 5′-CCCCGGTCCCGTTTTTAGATT-3′
	Reverse 5′-TCAGGCTCGGAGAATGATACA-3′
GAPDH	Forward 5′-GCTCCATTAGCCAAGGTTATTC-3′
	Reverse 5′-CAGCACCTCTACCATCTCTCC-3′

2.6. OS cell migration determination

The OS cell migration ability was determined using the wound abrasion assay. Briefly, a 200-μL pipette tip was scratched to create a straight wound when OS cells in 6-well plates after transfection reached >90% confluence. After washing twice with PBS, OS cells were incubated for 24 h. Images of the wound closure at 0 and 24 h were captured using a light microscope.

2.7. OS cell invasion detection

The Transwell assay was used to detect OS cell invasion. Transfected OS cells cultured in serum-free medium were added to an upper chamber precoated with Matrigel. Moreover, medium +10% FBS was added to the bottom chambers. After 24 h of incubation, OS cells reaching the underside of the chamber were fixed in 4% paraformaldehyde, stained with crystal violet, and counted under a light microscope.

2.8. Methylated RNA immunoprecipitation quantitative polymerase chain reaction (MeRIP-qPCR) assay

An MeRIP m^6A Kit (17-10499, Millipore, USA) was purchased to conduct a MeRIP-qPCR assay to analyze UBE3A m^6A levels. The RNA isolated from transfected OS cells was fragmented into 100 nucleotides and immunoprecipitated with magnetic beads coated with anti-IgG or anti-m^6A. After washing with IP buffer, immunopurified mRNAs were collected for qRT-PCR.

2.9. Western blotting

To isolate total proteins, RIPA Lysis Buffer (RM02998, ABclonal, China) was added to transfected OS cells. Then, the protein after detecting protein concentration by the BCA kit (Beyotime, China) was separated by sodium dodecyl sulfate polyacrylamide gel electrophoresis, transferred to polyvinylidene fluoride membranes, blocked with 5% nonfat milk, and incubated with the following antibodies: anti-UBE3A (A1757, ABclonal), anti-GAPDH (AC001, ABclonal), anti-Notch1 (A19090, ABclonal), and anti-HES1 (A0925, ABclonal). After incubating with the rabbit antibody, the protein was visualized using an ECL Super Kit (ABclonal).

2.10. RNA stability assay

To assess UBE3A mRNA stability after METTL16 knockdown, U2OS and HOS cells were transfected with si-METTL16 and incubated with actinomycin D (Sigma, USA) for 0, 2, 4, or 6 h. At each timepoint, the cells were collected to isolate RNA and perform qRT-PCR to detect the remaining mRNAs of UBE3A.

2.11. Luciferase assay

The UBE3A wild-type vector (UBE3A-WT) with the m^6A site and UBE3A-mutant vector (UBE3A-Mut) without the m^6A site were constructed by GenScript (China) and co-transfected with si-METTL16 into U2OS and HOS cells. After 24 h of incubation, luciferase activity was detected using a Dual-Luciferase Reporter Assay Kit (Promega, USA) according to the manufacturer's protocol.

2.12. RNA-binding protein immunoprecipitation (RIP) assay

A total of 1×10^7 U2OS and HOS cells were collected after centrifugation at 1500 rpm for 5 min at 4°C. Then, the RIP assay was performed by incubating with magnetic beads conjugated with 5 μg anti-IgG antibody or anti-FMR1 antibody using Magna RIP Kit (Merck, USA). After immunoprecipitation, UBE3A enrichment was examined by qRT-PCR.

2.13. Animal assay

UBE3A overexpression lentiviral vector and METTL16 knockdown lentiviral vector were constructed by GenScript (China) and transfected into HOS cells. BALB/c nude mice (male and 5 weeks old) from Huafukang Bioscience (China) were subcutaneously injected with 1×10^6 transfected HOS cells. The tumor volume was measured every week. After 4 weeks, the mice were euthanized to remove tumors for further measurement of the tumor weight and perform immunohistochemistry (IHC) to detect UBE3A and Ki-67 levels. The animal assay was approved by the ethics committee of Wuhan Third Hospital.

2.14. Statistical analysis

GraphPad Prism 10.1.2 was used for the statistical analysis of all data, which are shown as mean ± standard deviation from three repeated assays. Two-tailed t-tests or one-way analysis of variance was applied to compare differences between two or multiple groups. $^*p < 0.05$ and $^{**}p < 0.001$ indicate significance.

3. Results

3.1. METTL16 with high expression in OS

According to the data from the TNMplot platform, METTL16 was upregulated in the OS samples (Fig. 1A). Then, qRT-PCR was used to analyze METTL16 expression in OS cells (U2OS and HOS) and human osteoblast cell line hFOB1.19, revealing METTL16 upregulation in OS cells (Fig. 1B). These results demonstrate the high METTL16 expression in OS.

3.2. METTL16 depletion suppresses OS cell malignancy

To verify the function of METTL16 in OS cells, two siRNAs targeting METTL16 (si-METTL16#1 and si-METTL16#2) were first transfected into OS cells to silence METTL16 expression. qRT-PCR showed that si-METTL16#1 and si-METTL16#2 induced a >70% decrease in METTL16 levels in OS cells (Fig. 2A). Then, a series of cell functional experiments including CCK8 scratch and Transwell invasion assays were performed in transfected OS cells to assess cell proliferation, migration, and invasion. As shown in Fig. 2B, METTL16 knockdown effectively impaired cell proliferation ability in OS cells. Regarding cell migration, METTL16 knockdown reduced the cell migratory rate in OS cells (Fig. 2C). The number of invasive OS cells was also reduced in the two METTL16 knockdown groups (Fig. 2D). All data confirmed that OS cell malignancy could be inhibited by METTL16 knockdown.

3.3. METTL16 mediates UBE3A m^6A methylation in OS cells in a FMR1-dependent manner

To confirm the downstream target of METTL16 in OS, the TNMplot platform was first used to predict METTL16-correlated genes in OS. Meanwhile, the upregulated DEGs in the OS samples were screened from GSE16088 by setting the following screening criteria: $\log_2FC > 2$ and adj. $p < 0.01$. Using Venny 2.1, two common genes (UBE3A and SON) overlapped with GSE16088 and TNMplot (Fig. 3A). In qRT-PCR, only UBE3A expression was downregulated in OS cells after transfection with si-METTL16#1 and si-

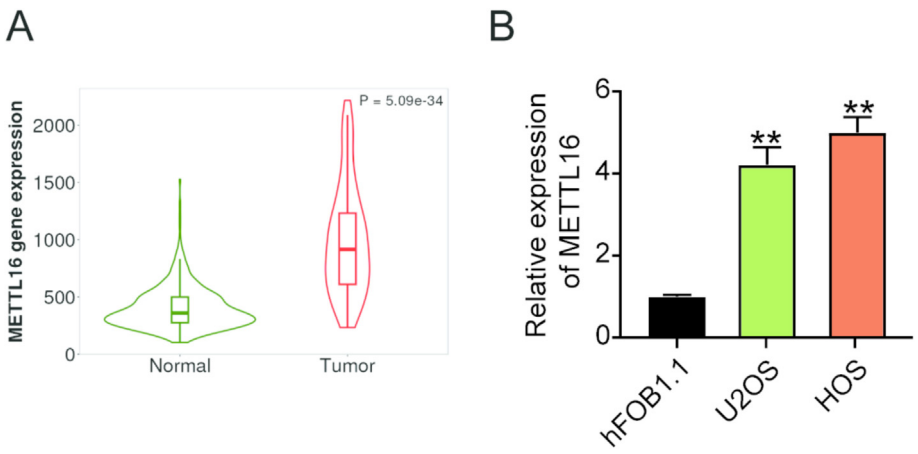

Fig. 1. METTL16 was highly expressed in OS. (A) The TNMplot platform was used to verify METTL16 expression in OS and normal samples. (B) qRT-PCR analyzed METTL16 expression in two OS cell lines (U2OS and HOS) and the normal osteoblast cell line hFOB1.19. $^{**}p < 0.001$ vs. hFOB1.19. n = 3 per group. Each experiment was replicated three times independently. Data are presented as mean ± SD. Significance was determined using one-way ANOVA.

METTL16#2 (Fig. 3B). Therefore, UBE3A was selected as the downstream target gene of METTL16 in OS for further exploration. The MeRIP-qPCR assay confirmed that the m^6A levels of UBE3A were inhibited in OS cells after transfection with si-METTL16#1 and si-METTL16#2 (Fig. 3C). The results of Western blotting displayed that METTL16 knockdown reduced UBE3A protein levels in OS cells (Fig. 3D). After actinomycin D treatment, UBE3A mRNA stability was impaired by MEETTL16 knockdown (Fig. 3E). RMBase v2.0 predicted a potential m^6A-modified site of UBE3A, and UBE3A wild-type/mutant (WT/Mut) vectors were constructed to perform luciferase assays according to the predicted site (Fig. 3F). The results of the luciferase assay indicated that METTL16 knockdown reduced luciferase activity in the UBE3A-WT group, whereas it did not affect luciferase activity in the UBE3A-Mut group (Fig. 3G). To further analyze the m^6A reader protein participating in METTL16-mediated UBE3A m^6A methylation, the RIP assay was performed, showing that the m6A reader protein FMR1 could bind to UBE3A in OS cells (Fig. 3H), and METTL16 knockdown reduced the binding ability between FMR1 and UBE3A (Fig. 3I). Taken together, the results of bioinformatics analysis and experiments confirmed that METTL16 mediates UBE3A m^6A methylation by the m^6A reader protein FMR1 in OS cells.

3.4. The promotive effects of UBE3A on OS cell malignancy are partly relieved by METTL16 knockdown via the Notch pathway

After transfecting UBE3A overexpression vectors and si-METTL16 into OS cells, the CCK8 assay revealed that UBE3A overexpression enhanced OS cell proliferation, whereas si-METTL16 impaired this promotive effect (Fig. 4A). The wound scratch assay revealed that UBE3A overexpression increased the OS cell migratory rate, whereas METTL16 knockdown partly reduced it because of UBE3A overexpression (Fig. 4B). Similarly, data from the Transwell invasion assay also revealed that the increase in the number of OS invasive cells induced by UBE3A overexpression was decreased by METTL16 knockdown (Fig. 4C). Moreover, Western blotting assay found that UBE3A overexpression enhanced the protein levels of Notch-1 and HES1 (key proteins of the Notch pathway) expression in OS cells. However, METTL16 knockdown partly reversed this positive effect on the expression of the key proteins of the Notch pathway (Fig. 4D). The above results demonstrated that UBE3A overexpression enhanced OS cell malignancy by activating the Notch pathway, whereas METTL16 knockdown partly relieved the effects of UBE3A overexpression.

3.5. UBE3A enhances OS cell malignancy via the Notch pathway

To verify whether UBE2C could exert an oncogenic role in OS cells via the Notch pathway, the Notch inhibitor DAPT was used to treat OS cells. The CCK8 assay showed that UBE3A overexpression-induced cell proliferation was inhibited by DAPT (Fig. 5A). The wound abrasion assay revealed that the high cell migratory rate caused by UBE3A overexpression was reduced by DAPT (Fig. 5B). The Transwell assay showed that DAPT inhibited the promotive effect of UBE3A overexpression on cell invasion (Fig. 5C). These findings indicate that UBE3A induces OS cell malignancy via the Notch pathway.

3.6. The positive effect of UBE3A on OS tumor growth is partly relieved by METTL16 knockdown

The effects of UBE3A interaction with METTL16 on tumor growth were explored in *in vivo* experiments. The tumor volume and size were larger in the UBE3A overexpression group than in empty vector group (Fig. 6A and Fig. 6B). However, METTL16 knockdown partly reduced the tumor volume and size induced by UBE3A overexpression. By tumor weight, UBE3A overexpression increased the tumor weight, whereas METTL16 knockdown partly decreased the tumor weight induced by UBE3A overexpression (Fig. 6C). IHC results showed that UBE3A overexpression induced the upregulation of UBE3A and Ki-67, whereas METTL16 knockdown reduced the upregulation of UBE3A and Ki-67 (Fig. 6D). Overall, *in vivo* experiments showed that UBE3A overexpression facilitated tumor growth; however, METTL16 knockdown partly relieved this promotive effect of UBE3A overexpression.

4. Discussion

OS remains one of the most aggressive and therapy-resistant malignancies, with limited improvements in clinical outcomes over the past decades [21,22]. Complex and multifactorial molecular mechanisms drive OS progression, necessitating the identification of novel therapeutic targets. In this study, METTL16, a critical m^6A methyltransferase, was upregulated in OS and promoted OS malignancy. Further investigation revealed that METTL16 induced m^6A methylation of UBE3A mRNA to enhance UBE3A expression via the m^6A reader protein FMR1, thereby activating the Notch signaling pathway. Our results reveal that a previously unrecognized m^6A methylation mechanism involved the METTL16/UBE3A axis in

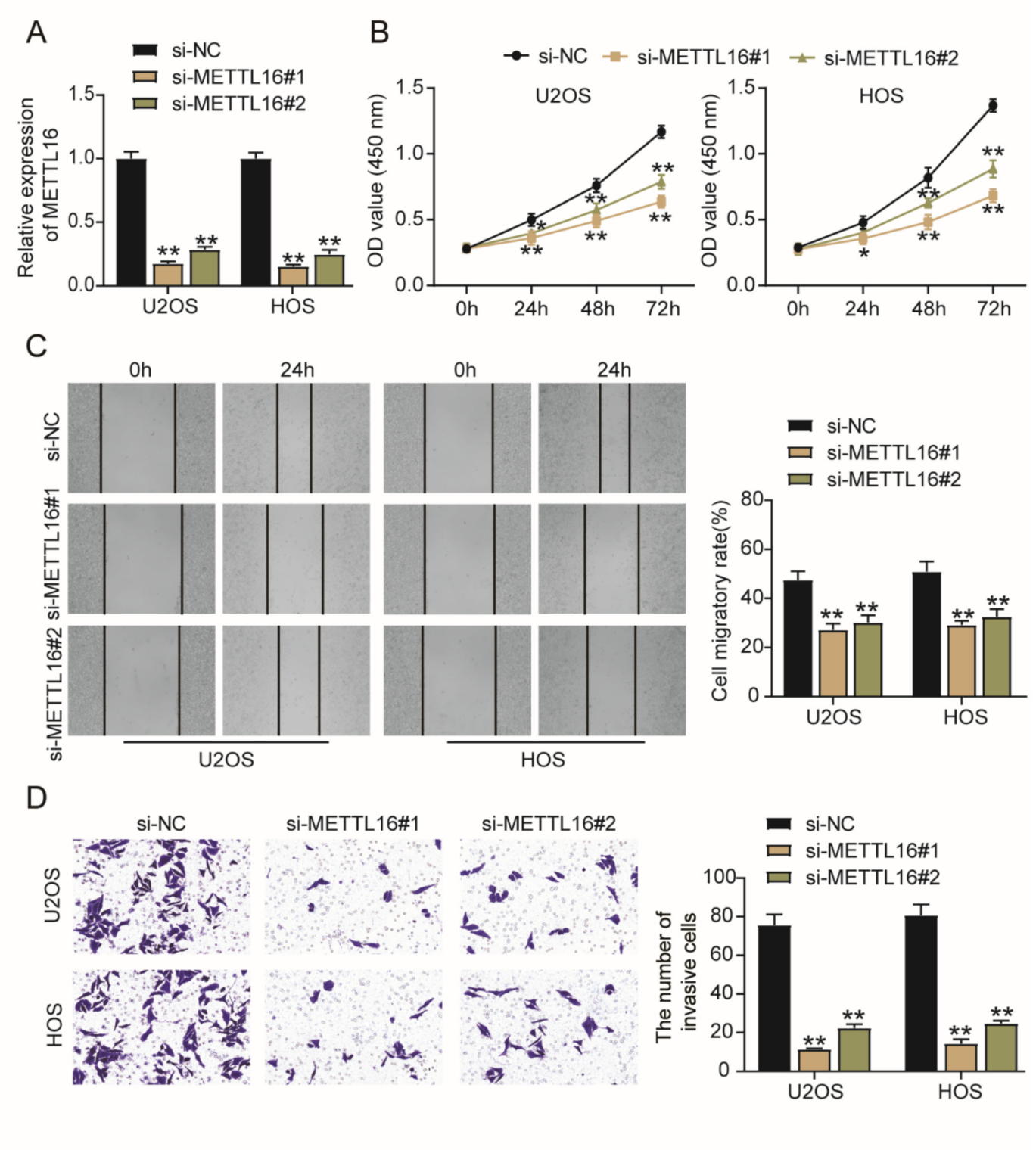

Fig. 2. METTL16 knockdown suppresses OS cell malignancy. (A) qRT-PCR detected the transfection efficiency of two siRNAs targeting METTL16 (si-METTL16#1 and si-METTL16#2) transfected into OS cells. (B) CCK8 assay was performed to assess transfected OS cell proliferation ability. (C) Scratch assay was performed to detect transfected OS cell migration ability. (D) Transwell invasion assay determined the number of transfected OS invasive cells. $^{*}p < 0.05$, $^{**}p < 0.001$ vs. si-NC. n = 3 per group. Each experiment was replicated three times independently. Data are presented as mean ± SD. Significance was determined using one-way ANOVA.

OS, which may provide new insights into the pathogenesis and potential therapeutic strategies for OS.

This study revealed METTL16 upregulation in OS, indicating its key role in OS progression. The function of METTL16 in cancer has been increasingly implicated in numerous studies. For instance, METTL16 is upregulated in gastric cancer and promotes tumor growth by regulating m^{6}A methylation of cyclin D1 to enhance cyclin D1 stability [23]. However, METTL16 was downregulated in papillary thyroid cancer to restrain tumorigenesis by increasing the m^{6}A level of SCD1 mRNA [24]. Previous studies have shown

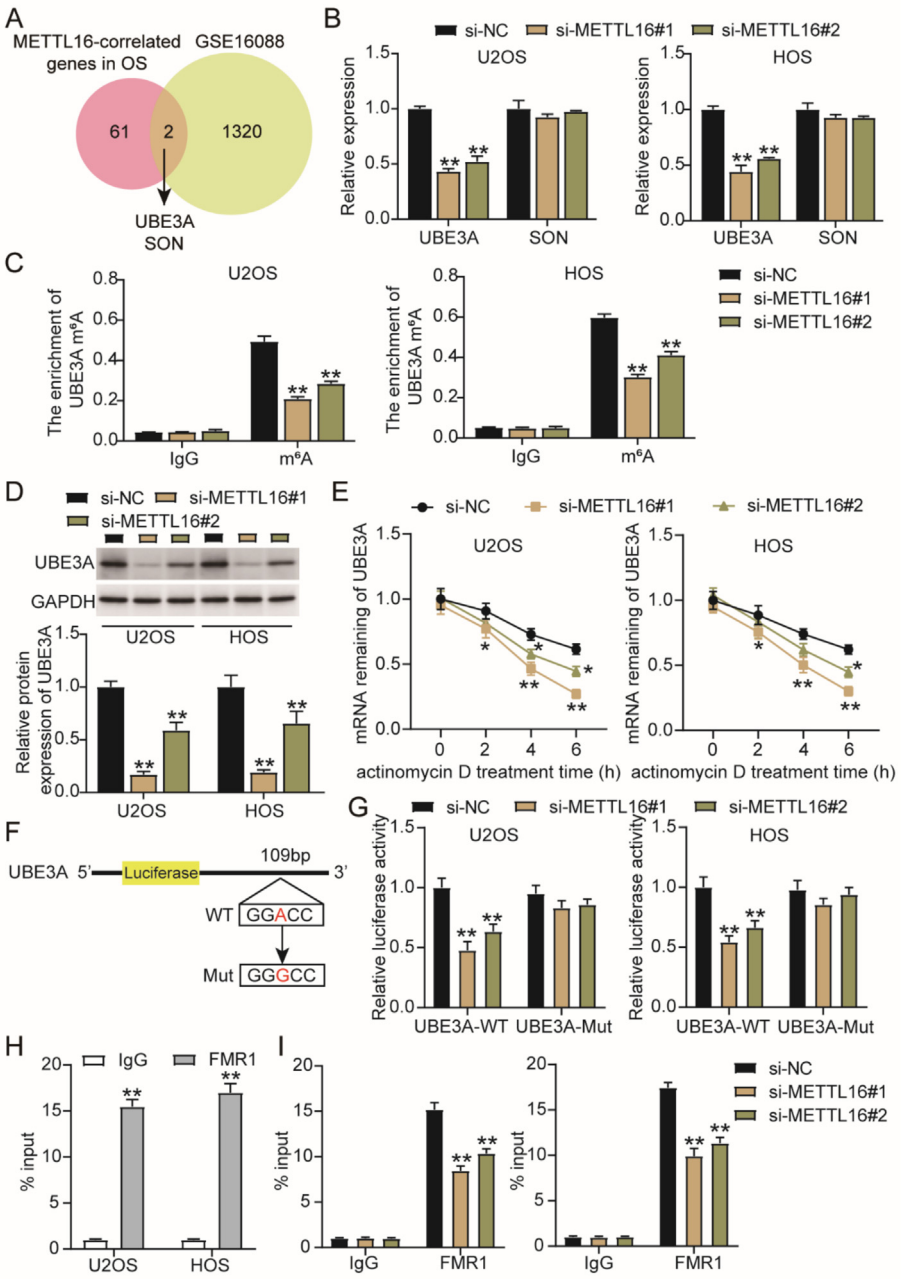

Fig. 3. METTL16 mediates m^{6}A methylation of UBE3A in OS cells in a FMR1-dependent manner. (A) Venny 2.1 overlapped the common genes from GSE16088 and TNMplot. GSE16088, an mRNA microarray, was used to screen the upregulated DEGs in OS samples with $\log_2$FC > 2 and adj. $p < 0.01$. TNMplot predicted the METTL16-correlated genes in OS. (B) qRT-PCR detected the expression of UBE3A and SON in OS cells after si-METTL16#1 and si-METTL16#2 transfection. (C) MeRIP-qPCR assay measured the m^{6}A levels of UBE3A in OS cells after si-METTL16#1 and si-METTL16#2 transfection. (D) Western blotting assessed the levels of UBE3A protein in OS cells after si-METTL16#1 and si-METTL16#2 transfection. (E) RNA stability assay detected UBE3A mRNA stability in OS cells after si-METTL16#1 and si-METTL16#2 transfection. (F) RMBase v2.0 predicted the m^{6}A-modified site of UBE3A. (G) Luciferase assay measured the luciferase activity in OS cells after co-transfection of UBE3A wild-type/mutant vectors (UBE3A-WT/UBE3A-Mut) and si-METTL16#1/si-METTL16#2. (H) The RIP assay detected the enrichment of UBE3A binding to FMR1. (I) The RIP assay detected the effect of METTL16 knockdown on the binding of FMR1 and UBE3A in OS cells. $^*p < 0.05$, $^{**}p < 0.001$ vs. si-NC or IgG. n = 3 per group. Each experiment was replicated three times independently. Data are presented as mean ± SD. Significance was determined using two-tailed t-tests for two groups and one-way ANOVA for multiple groups.

that METTL16 plays dual roles in cancer, depending on the specific tumor type. In OS, only one study revealed METTL16 upregulation in OS to promote OS progression by regulating m^{6}A modification of VPS33B [25]. Consistent with previous findings, the present study also showed that METTL16 upregulation in OS plays an oncogenic role. However, UBE3A was the downstream of METTL16, and METTL16 induced the m^{6}A methylation of UBE3A to enhance UBE3A expression and mRNA stability via the m^{6}A reader protein FMR1 in OS.

UBE3A, an E3 ubiquitin ligase best known for its role in Angelman syndrome, has recently emerged as a tumor-progression regulator. For example, Zhang et al. [19] used the data of non-small-cell lung cancer samples from TCGA and GEO databases to prove that UBE3A deletion enhanced the efficiency of immunotherapy, indicating that UBE3A is an oncogene in lung cancer. Zheng et al. [20] revealed that a high UBE3A expression in esophageal cancer could promote esophageal cancer cell malignancy via bioinformatic analysis and *in vivo* and *in vitro* experiments. However, a

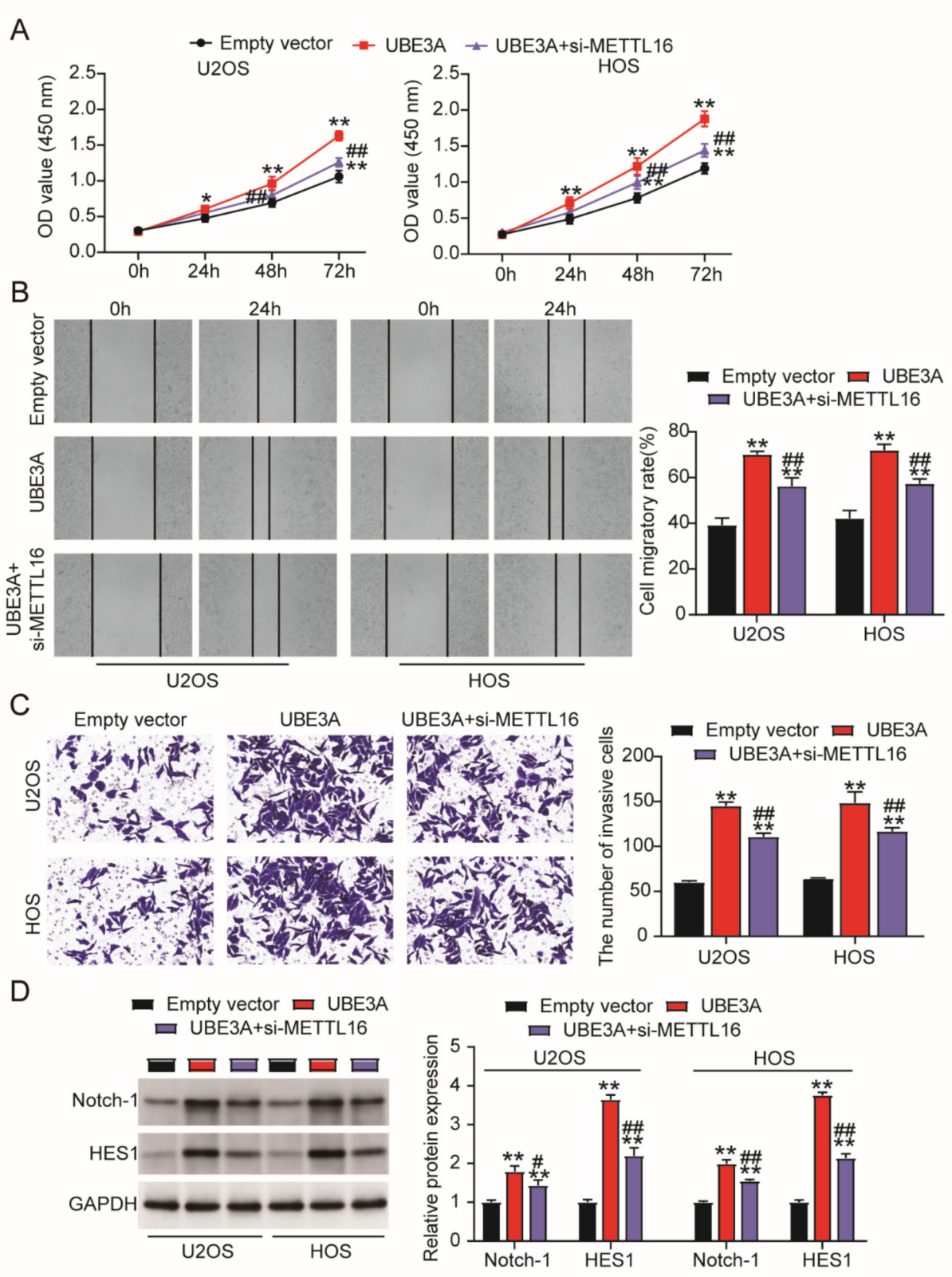

Fig. 4. The promotive effects of UBE3A on OS cell malignancy are partly relieved by METTL16 knockdown via the Notch pathway. (A) The CCK8 assay assessed the proliferation ability in OS cells after the transfection of UBE3A overexpression vector and si-METTL16. (B) The wound scratch assay detected migration ability in OS cells after the transfection of UBE3A overexpression vector and si-METTL16. (C) The Transwell invasion assay determined invasion in OS cells after the transfection of UBE3A overexpression vector and si-METTL16. (D) Western blotting detected the key proteins of the Notch pathway in OS cells after the transfection of UBE3A overexpression vector and si-METTL16. UBE3A, UBE3A overexpression vector. $^{*}p < 0.05$, $^{**}p < 0.001$ against empty vector; $^{\#}p < 0.05$, $^{\#\#}p < 0.001$ vs. UBE3A. n = 3 per group. Each experiment was replicated three times independently. Data are presented as mean ± SD. Significance was determined using one-way ANOVA.

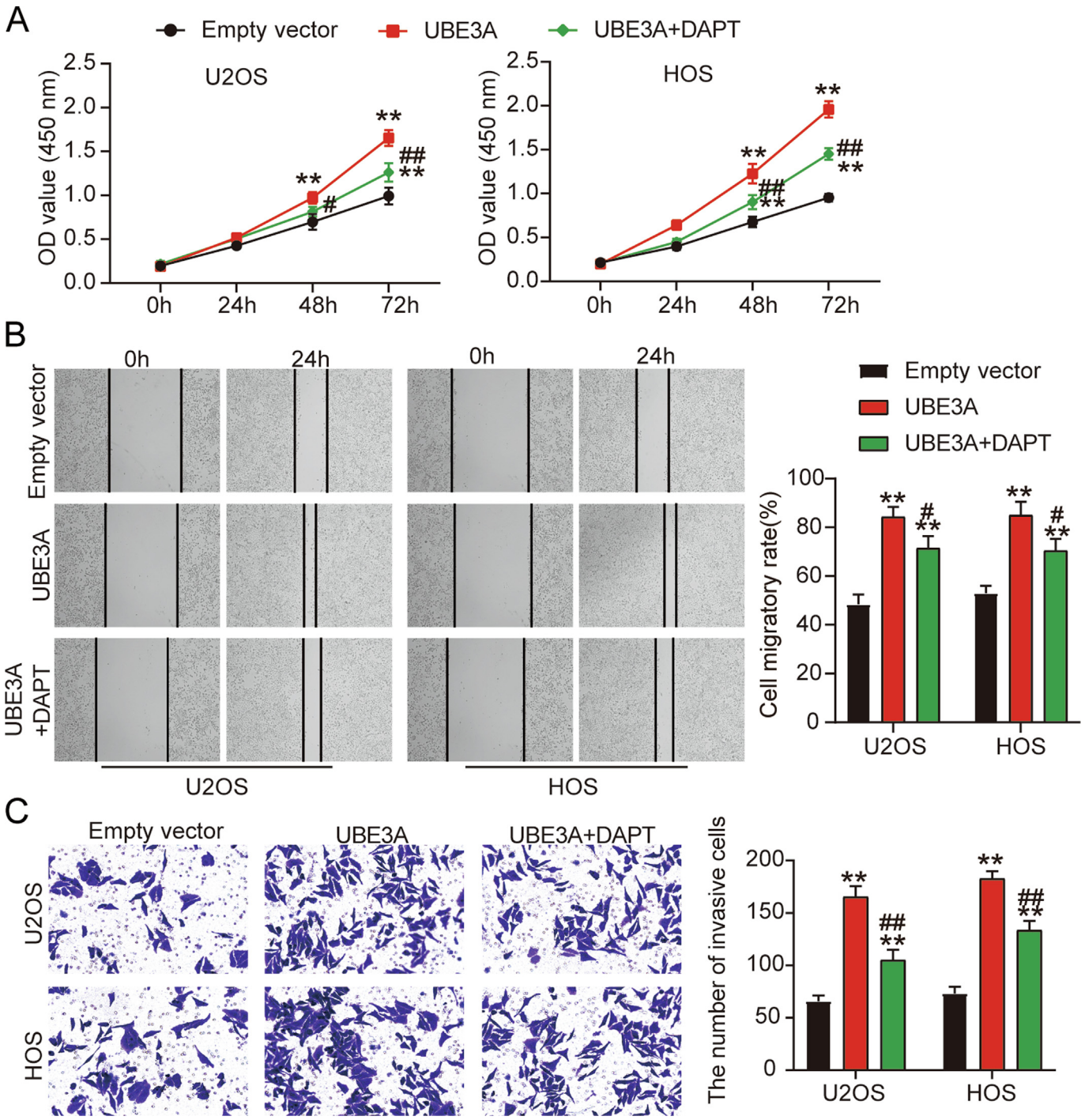

Fig. 5. UBE3A enhances OS cell malignancy via the Notch pathway. (A) The Cell Counting Kit-8 (CCK8) assay assessed the proliferation ability in OS cells after the transfection with a UBE3A overexpression vector and DAPT treatment. (B) The wound scratch assay detected migration ability in OS cells after the transfection of UBE3A overexpression vector and DAPT treatment. (C) The Transwell invasion assay determined invasion in OS cells after the transfection of UBE3A overexpression vector and DAPT treatment. $^{**}p < 0.001$ vs. empty vector; $^{\#}p < 0.05$, $^{\#\#}p < 0.001$ vs. UBE3A. n = 3 per group. Each experiment was replicated three times independently. Data are presented as mean ± SD. Significance was determined using one-way ANOVA.

study revealed the role of UBE3A in OS. Here, bioinformatics analysis was conducted to confirm the upregulation of UBE3A expression in OS. After performing *in vivo* and *in vitro* experiments, this study proved for the first time that UBE3A overexpression facilitated OS tumorigenesis by activating the Notch signaling pathway.

The Notch signaling pathway, a highly conserved cell–cell communication pathway, is crucial in regulating cell fate, proliferation, differentiation, and apoptosis [26,27,28]. In cancer, the Notch signaling pathway acts as either an oncogene or tumor suppressor, depending on the tissue type and cellular environment. For example, the Notch signaling pathway is aberrantly activated in various malignancies, including hepatocellular carcinoma, breast cancer, and colorectal cancer, where it promotes tumor growth, angiogenesis, and metastasis [29,30,31]. Conversely, the Notch signaling pathway exerts tumor-suppressive effects on acute megakaryoblastic leukemia by impeding proliferation [32]. In OS, the activa-

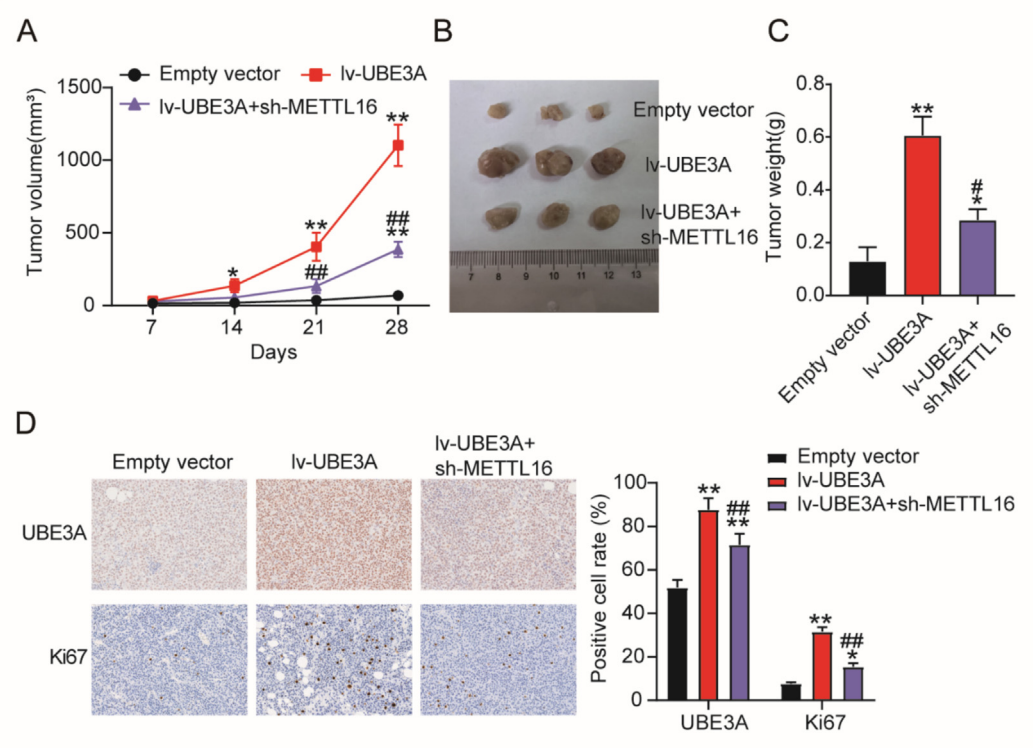

Fig. 6. The positive effect of UBE3A on OS tumor growth is partly relieved by METTL16 knockdown. (A) Tumor volume from HOS cell-injected nude mice transfected with UBE3A overexpression and METTL16 knockdown lentiviral vector. (B) Tumor from the nude mice injected with HOS cells transfected with UBE3A overexpression and METTL16 knockdown lentiviral vector. (C) Tumor weight from the nude mice injected with HOS cells transfected with UBE3A overexpression and METTL16 knockdown lentiviral vector. lv-UBE3A, UBE3A overexpression lentiviral vector. sh-METTL16, METTL16 knockdown lentiviral vector. (D) IHC detected the levels of UBE3A and Ki-67 in tumors from nude mice injected with HOS cells transfected with UBE3A overexpression and METTL16 knockdown lentiviral vector. lv-UBE3A, UBE3A overexpression lentiviral vector. sh-METTL16 and METTL16 knockdown lentiviral vector. $^{*}p < 0.05$, $^{**}p < 0.001$ vs. empty vector; $^{\#}p < 0.05$, $^{\#\#}p < 0.001$ vs. lv-UBE3A. n = 3 per group. Each experiment was replicated three times independently. Data are presented as mean ± SD. Significance was determined using one-way ANOVA.

tion of the Notch signaling pathway, regulated by CEMIP, DLX5, and BMP9, promotes OS progression [33,34,35]. To our knowledge, this study is the first to reveal that UBE3A in OS induces the activation of the Notch signaling pathway by enhancing Notch-1 protein expression, thereby playing an oncogenic role in OS.

This study explored the function of the METTL16/UBE3A/Notch signaling pathway axis in OS; however, some limitations should be resolved in the future. First, this study identified UBE3A and SON as downstream candidates of METTL16 through integrative analysis of the GSE16088 and TNMplot datasets. Further experiments showed that METTL16 knockdown partially reversed the oncogenic effect of UBE3A on OS progression. Our selection strategy emphasized stringent differential expression and correlation to increase confidence; however, this may have excluded moderately regulated or noncoding m^{6}A-modified transcripts. Therefore, future studies incorporating m^{6}A-RNA immunoprecipitation sequencing (m^{6}A-RIP-seq) or cross-linking immunoprecipitation sequencing (CLIP-seq) are critical to further delineate the complete METTL16 target landscape and validate its functional relevance in OS progression. Second, in addressing the molecular mechanism by which UBE3A regulates Notch signaling, prior literatures were reviewed, which revealed that only Zheng et al. reported that UBE3A could activate Notch signaling in esophageal cancer by promoting ZNF185 degradation [20]. However, in the present study, ZNF185 expression did not change in OS cells after UBE3A overexpression (data not shown), indicating a potentially distinct mechanism in OS. Further investigation, such as proteomic screening to identify alternative substrates or interactors of UBE3A, is warranted to clarify the molecular mechanism by which UBE3A activates Notch signaling in OS. In addition, owing to the limited clinical samples, the correlation between METTL16 expression and prognosis could not be analyzed in the present study. In the future, more clinical OS samples should be collected to explore the clinical value of METTL16.

In conclusion, this study established METTL16 as a tumor promotor in OS progression by modulating UBE3A expression via m^{6}A methylation to activate the Notch signaling pathway. These findings not only expand the mechanistic understanding of m^{6}A regulatory mechanism in OS but also highlight the therapeutic potential of disrupting the METTL16–UBE3A–Notch pathway axis in OS.

CRediT authorship contribution statement

Yanlin Tan: Writing – original draft, Formal analysis, Investigation, Conceptualization, Methodology, Data curation. **Jun Gao:** Writing – review & editing.

Ethical approval (animals)

The Ethics Committee of Wuhan Third Hospital approved the animal study, which was executed according to the ARRIVE guidelines.

Financial support

This research did not receive any specific grant from funding agencies in the public, commercial, or not-for-profit sectors.

Declaration of competing interest

No conflicts of interest were declared by the authors.

Supplementary material

https://doi.org/10.1016/j.ejbt.2025.07.006.

Data availability

Data will be made available on request.

References

[1] Kim C, Davis LE, Albert CM, et al. Osteosarcoma in pediatric and adult populations: Are adults just big kids? Cancers 2023;15(20):5044. https://doi.org/10.3390/cancers15205044. PMid: 37894411.

[2] Yu S, Yao X. Advances on immunotherapy for osteosarcoma. Mol Cancer 2024;23(1):192. https://doi.org/10.1186/s12943-024-02105-9. PMid: 39245737.

[3] Harris MA, Hawkins CJ. Recent and ongoing research into metastatic osteosarcoma treatments. Int J Mol Sci 2022;23(7):3817. https://doi.org/10.3390/ijms23073817. PMid: 35409176.

[4] Lilienthal I, Herold N. Targeting molecular mechanisms underlying treatment efficacy and resistance in osteosarcoma: A review of current and future strategies. Int J Mol Sci 2020;21(18):6885. https://doi.org/10.3390/ijms21186885. PMid: 32961800.

[5] Sheng G, Gao Y, Yang Y, et al. Osteosarcoma and metastasis. Front Oncol. 2021;11:780264. https://doi.org/10.3389/fonc.2021.780264. PMid: 34956899.

[6] Moukengue B, Lallier M, Marchandet L, et al. Origin and therapies of osteosarcoma. Cancers 2022;14(14):3503. https://doi.org/10.3390/cancers14143503. PMid: 35884563.

[7] Uddin MB, Wang Z, Yang C. The m^{6}A RNA methylation regulates oncogenic signaling pathways driving cell malignant transformation and carcinogenesis. Mol Cancer 2021;20(1):61. https://doi.org/10.1186/s12943-021-01356-0. PMid: 33814008.

[8] Wang Y, Wang Y, Patel H, et al. Epigenetic modification of m^{6}A regulator proteins in cancer. Mol Cancer 2023;22(1):102. https://doi.org/10.1186/s12943-023-01810-1. PMid: 37391814.

[9] He PC, He C. m^{6}A RNA methylation: From mechanisms to therapeutic potential. EMBO J 2021;40(3):e105977. https://doi.org/10.15252/embj.2020105977. PMid: 33470439.

[10] Wang S, Lv W, Li T, et al. Dynamic regulation and functions of mRNA m6A modification. Cancer Cell Int 2022;22(1):48. https://doi.org/10.1186/s12935-022-02452-x. PMid: 35093087.

[11] Zhang J, Tong L, Liu Y, et al. The regulatory role of m^{6}A modification in the maintenance and differentiation of embryonic stem cells. Genes Dis. 2024;11(5):101199. https://doi.org/10.1016/j.gendis.2023.101199. PMid: 38947741.

[12] Petri BJ, Klinge CM. m6A readers, writers, erasers, and the m6A epitranscriptome in breast cancer. J Mol Endocrinol 2023;70(2):e220110. https://doi.org/10.1530/JME-22-0110. PMid: 36367225.

[13] Yao Y, Liu P, Li Y, et al. Regulatory role of m^{6}A epitranscriptomic modifications in normal development and congenital malformations during embryogenesis. Biomed Pharmacother 2024;173:116171. https://doi.org/10.1016/j.biopha.2024.116171. PMid: 38394844.

[14] Ye F, Wu J, Zhang F. METTL16 epigenetically enhances GPX4 expression via m6A modification to promote breast cancer progression by inhibiting ferroptosis. Biochem Biophys Res Commun 2023;638:1–6. https://doi.org/10.1016/j.bbrc.2022.10.065. PMid: 36434904.

[15] Yi T, Wang C, Ye X, et al. METTL16 inhibits pancreatic cancer proliferation and metastasis by promoting MROH8 RNA stability and inhibiting CAPN2 expression - experimental studies. Int J Surg 2024;110(12):7701–19. https://doi.org/10.1097/JS9.0000000000002116. PMid: 39434688.

[16] Chaudhary P, Proulx J, Park IW. Ubiquitin-protein ligase E3A (UBE3A) mediation of viral infection and human diseases. Virus Res 2023;335:199191. https://doi.org/10.1016/j.virusres.2023.199191. PMid: 37541588.

[17] Zhu J, Tsai NP. Ubiquitination and E3 ubiquitin ligases in rare neurological diseases with comorbid epilepsy. Neuroscience 2020;428:90–9. https://doi.org/10.1016/j.neuroscience.2019.12.030. PMid: 31931110.

[18] Jan M, Sperling AS, Ebert BL. Cancer therapies based on targeted protein degradation - lessons learned with lenalidomide. Nat Rev Clin Oncol 2021;18(7):401–17. https://doi.org/10.1038/s41571-021-00479-z. PMid: 33654306.

[19] Zhang N, Shen J, Gou L, et al. UBE3A deletion enhances the efficiency of immunotherapy in non-small-cell lung cancer. Bioengineered. 2022;13(5):11577–92. https://doi.org/10.1080/21655979.2022.2069328. PMid: 35531878.

[20] Zheng Z, Zhang B, Yu H, et al. UBE3A activates the NOTCH pathway and promotes esophageal cancer progression by degradation of ZNF185. Int J Biol Sci 2021;17(12):3024–35. https://doi.org/10.7150/ijbs.61117. PMid: 34421347.

[21] Isakoff MS, Bielack SS, Meltzer P, et al. Osteosarcoma: Current treatment and a collaborative pathway to success. J Clin Oncol 2015;33(27):3029–35. https://doi.org/10.1200/JCO.2014.59.4895. PMid: 26304877.

[22] Tian H, Cao J, Li B, et al. Managing the immune microenvironment of osteosarcoma: The outlook for osteosarcoma treatment. Bone Res 2023;11(1):11. https://doi.org/10.1038/s41413-023-00246-z. PMid: 36849442.

[23] Wang XK, Zhang YW, Wang CM, et al. METTL16 promotes cell proliferation by up-regulating cyclin D1 expression in gastric cancer. J Cell Mol Med 2021;25(14):6602–17. https://doi.org/10.1111/jcmm.16664. PMid: 34075693.

[24] Li Q, Wang Y, Meng X, et al. METTL16 inhibits papillary thyroid cancer tumorigenicity through m^{6}A/YTHDC2/SCD1-regulated lipid metabolism. Cell Mol Life Sci 2024;81(1):81. https://doi.org/10.1007/s00018-024-05146-x. PMid: 38334797.

[25] Cheng J, Xu Z, Tan W, et al. METTL16 promotes osteosarcoma progression by downregulating VPS33B in an m^{6}A-dependent manner. J Cell Physiol 2024;239(3):e31068. https://doi.org/10.1002/jcp.31068. PMid: 37357526.

[26] Shi Q, Xue C, Zeng Y, et al. Notch signaling pathway in cancer: From mechanistic insights to targeted therapies. Signal Transduct Target Ther 2024;9(1):128. https://doi.org/10.1038/s41392-024-01828-x. PMid: 38797752.

[27] Li X, Yan X, Wang Y, et al. The Notch signaling pathway: A potential target for cancer immunotherapy. J Hematol Oncol 2023;16(1):45. https://doi.org/10.1186/s13045-023-01439-z. PMid: 37131214.

[28] Mashanov V, Akiona J, Khoury M, et al. Active Notch signaling is required for arm regeneration in a brittle star. PLoS One 2020;15(5):e0232981. https://doi.org/10.1371/journal.pone.0232981. PMid: 32396580.

[29] Zhan P, Lu Y, Lu J, et al. The activation of the Notch signaling pathway by UBE2C promotes the proliferation and metastasis of hepatocellular carcinoma. Sci Rep 2024;14(1):22859. https://doi.org/10.1038/s41598-024-72714-3. PMid: 39353974.

[30] Jiang N, Hu Y, Wang M, et al. The Notch signaling pathway contributes to angiogenesis and tumor immunity in breast cancer. Breast Cancer (Dove Med Press). 2022;14:291–309. https://doi.org/10.2147/BCTT.S376873. PMid: 36193236.

[31] Zhang T, Chen S, Peng Y, et al. NOVA1-Mediated SORBS2 isoform promotes colorectal cancer migration by activating the Notch pathway. Front Cell Dev Biol 2021;9:673873. https://doi.org/10.3389/fcell.2021.673873. PMid: 34692669.

[32] Ong KOK, Mok MMH, Niibori-Nambu A, et al. Activation of NOTCH signaling impedes cell proliferation and survival in acute megakaryoblastic leukemia. Exp Hematol 2024;137:104255. https://doi.org/10.1016/j.exphem.2024.104255. PMid: 38876252.

[33] Cheng J, Zhang Y, Wan R, et al. CEMIP promotes osteosarcoma progression and metastasis through activating Notch signaling pathway. Front Oncol 2022;12:919108. https://doi.org/10.3389/fonc.2022.919108. PMid: 35957875.

[34] Zhang X, Bian H, Wei W, et al. DLX5 promotes osteosarcoma progression via activation of the NOTCH signaling pathway. Am J Cancer Res 2021;11(6):3354–74. PMid: 34249467.

[35] Liu P, Man Y, Wang Y, et al. Mechanism of BMP9 promotes growth of osteosarcoma mediated by the Notch signaling pathway. Oncol Lett 2016;11(2):1367–70. https://doi.org/10.3892/ol.2015.4067. PMid: 26893744.